Classification of Ethylene–Styrene Interpolymers Based on Comonomer Content

H. CHEN,[1] M. J. GUEST,[2] S. CHUM,[2] A. HILTNER,[1] E. BAER[1]

[1]Department of Macromolecular Science and Center for Applied Polymer Research, Case Western Reserve University, Cleveland, Ohio 44106-7202

[2]Polyethylene and INSITE™ Technology R & D, The Dow Chemical Company, Freeport, Texas 77541-3257

Received 21 January 1998; accepted 3 March 1998

ABSTRACT: Copolymerization of ethylene and styrene by the INSITE™ technology from Dow presents a new polymer family identified as ethylene–styrene interpolymers (ESI). Based on the combined observations from melting behavior, density, dynamic mechanical response, and tensile deformation, a classification scheme with 3 distinct categories is proposed. Polymers with up to 50 wt % styrene are semicrystalline and are classified as type E. The stress–strain behavior of low-crystallinity polymers at ambient temperature exhibits elastomeric characteristics with low initial modulus, a gradual increase in the slope of the stress–strain curve at higher strains, and large instantaneous recovery. The structural origin of the elastomeric behavior is probably a network of flexible chains with fringed micellar crystals serving as multifunctional junctions. Polymers with more than 50 wt % styrene are amorphous. Because the range of glass transition temperatures encompasses ambient temperature (nominally 25°C), it is useful to differentiate ESIs that are above the glass transition as type M and those that are below the glass transition as type S. Type M polymers behave as rubber-like liquids. They have the lowest modulus and lowest stress levels. Some elastic characteristics are attributed to the entanglement network. Type S polymers exhibit large strain rate sensitivity with glassy behavior at short times and rubbery behavior at longer times. The term "glasstomer" is coined to describe these polymers. The division between type M and type S is based on chain dynamics, rather than solid state structure, and thus depends on the temperature of interest. At ambient temperature, ESIs with 50 to 70 wt % styrene are classified as type M; polymers with more than 70 wt % styrene are classified as type S. © 1998 John Wiley & Sons, Inc. J Appl Polym Sci 70: 109–119, 1998

Key words: polyethylene; ethylene–styrene copolymers; constrained geometry catalyst technology

INTRODUCTION

Despite the scientific and commercial appeal offered by copolymers of ethylene and styrene, attempts to copolymerize these monomers by free radical methods or conventional Ziegler–Natta catalysts have been generally unsuccessful, typically yielding mixtures of homopolymers.[1–3] Renewed interest in ethylene–styrene copolymerization has been generated by the development of metallocene and single site catalysts.[4–6] Recently, polymerization of ethylene and styrene by the INSITE™ technology from Dow has achieved polymers with up to 80 wt % styrene.[7–9]

Initial efforts to develop the new catalysts focused on copolymerization of ethylene with α-ole-

Correspondence to: A. Hiltner.

Journal of Applied Polymer Science, Vol. 70, 109–119 (1998)
 CCC 0021-8995/98/010109-11

Table I Ethylene–Styrene Copolymers

Designation	Total Styrene (wt %)	aPS (wt %)	Styrene[a] (wt %)	Styrene[b] (mol %)	$10^{-3}\ M_w$	M_w/M_n	Talc (wt %)
ES16	22.6	8.2	15.7	4.7	—	—	0
ES24	29.3	7.3	23.7	7.7	—	—	0
ES27	28.2	1.2	27.3	9.2	240.9	2.04	1.21
ES28	32.7	6.4	28.1	9.5	—	—	0
ES30	32.9	4.7	29.6	10.2	—	—	0
ES44	45.0	2.0	43.9	17.4	243.9	2.9	0
ES53	53.3	1.7	52.5	22.9	267.3	2.8	0
ES58	59.5	3.4	58.1	27.2	275.4	3.1	0
ES62	66.2	9.4	62.7	31.2	276.4	3.3	0
ES63	63.9	3.1	62.8	31.3	267.6	3.0	0
ES69	72.4	10.3	69.2	37.7	283.1	3.0	0
ES72	74.8	7.8	72.7	41.8	186.8	2.6	0
ES73	74.7	6.9	72.8	41.9	170.2	5.3	0
ES74	76.7	9.4	74.3	43.6	340.0	2.1	2.42

[a] Styrene in ESI: (total wt % styrene-wt % aPS)/(100-wt % aPS).
[b] From wt % styrene in ESI.

fins. Essentially, random comonomer incorporation created microstructures that differ significantly from conventional linear ethylene copolymers. The molecular weight distribution of the new copolymers is narrow, and the comonomer distribution is homogeneous. The control on molecular architecture makes it possible to produce homogeneous copolymers across a broad composition range. This opens up an opportunity to create unique families of polymers. With the wide range of properties exhibited, a concise relationship between solid-state structure and properties is desirable; classification based on comonomer content is then possible.

This approach was employed to describe ethylene–octene (EO) copolymers prepared by the INSITE™ technology from Dow.[10] These copolymers present a broad range of solid-state structures from highly crystalline, lamellar morphologies to fringed micellar morphologies of low crystallinity. Correspondingly, the tensile behavior of EO copolymers changes from necking and cold drawing typical of a semicrystalline thermoplastic to uniform extension and high recovery characteristic of an elastomer. Although changes in morphological features and tensile properties occur gradually with increasing comonomer content, the exceptionally large range in these characteristics makes a classification scheme with 4 distinct categories useful.

The copolymers of ethylene and styrene used in this study have substantially random incorporation of styrene except that successive head-to-tail styrene chain insertions are shown by ^{13}C nuclear magnetic resonance (^{13}C-NMR) analysis to be absent, even at high levels of styrene incorporation.[9] For this reason, the polymers are described as "pseudorandom" ethylene–styrene interpolymers (ESI). An initial characterization of ESIs over the composition range up to 50 mol % (80 wt %) styrene reveals a broad range of properties as the microstructure changes from crystalline to amorphous. These are conveniently categorized into 3 performance regimes.[7–9] The studies described here were undertaken to develop more concisely the relationship of composition to solid-state structure and properties. In contrast to the classification scheme of EO copolymers, which focused on semicrystalline polymers with less than 15 mol % comonomer, the present efforts emphasize the amorphous polymers.

EXPERIMENTAL

Materials

The ESIs synthesized by the INSITE™ technology from Dow are listed in Table I. The composition and molecular weight data in Table I were provided by Dow. The polymers contained a small amount of atactic styrene homopolymer (aPS). The total styrene and aPS as weight percents of total polymer were obtained by NMR. The poly-

Table II Properties of Ethylene–Styrene Interpolymers

Designation	Density (g/cc)	Crystallinity (%) (DSC) (Based on Copolymer)	T_g (°C) (DMTA, 1 Hz, tan δ)	Activation Energy of Glass Transition (kJ/mol)	Modulus[a] (MPa)	Fracture Stress[a] (MPa)	Fracture Strain[a] (%)
ES16	0.9420	37.5	12.7	n/a	52.8 ± 2.2	31.7 ± 2.3	666 ± 34
ES24	0.9445	26.6	0.0	n/a	26.4 ± 1.3	33.3 ± 2.4	517 ± 28
ES27	0.9355	17.4	−3.7	n/a	25.0 ± 2.6	29.9 ± 3.0	453 ± 23
ES28	0.9464	22.9	−4.0	282	19.5 ± 1.4	32.8 ± 1.6	564 ± 17
ES30	0.9454	19.6	−1.9	n/a	25.4 ± 1.4	32.0 ± 1.2	468 ± 14
ES44	0.9486	5.0	−9.4	256	3.2 ± 1.1	10.9 ± 0.3	576 ± 2
ES53	0.9678	n/a	−2.4	308	2.5 ± 0.3	<0.7	>2000
ES58	0.9810	n/a	5.9	318	2.7 ± 0.3	<0.7	>2000
ES62	0.9937	n/a	11.4	n/a	3.9 ± 0.0	5.9 ± 0.1	559 ± 9
ES63	0.9901	n/a	11.1	340	3.9 ± 0.4	2.9 ± 0.1	707 ± 39
ES69	1.0123	n/a	22.7	362	10.6 ± 2.5	21.2 ± 0.3	412 ± 4
ES72	1.0186	n/a	33.8	n/a	741 ± 83	22.8 ± 0.4	292 ± 5
ES73	1.0207	n/a	32.6	373	311 ± 16	14.4 ± 0.4	263 ± 3
ES74	1.0214	n/a	33.0	376	724 ± 201	25.8 ± 2.5	268 ± 32

[a] 100%/min strain rate.

mers are designated by the prefix ES, followed by the weight percent styrene.

Methods

Pellets were molded into plaques 1.3 mm thick and film 0.5 mm thick. The pellets were sandwiched between Mylar® sheets, heated at 190°C under minimal pressure for 5 min, under 276 psi pressure for 5 min, under 560 psi pressure for 1 min, and quenched in ice water. The plaques were used for thermogravimetric analysis (TGA), differential scanning calorimetry (DSC), density, and stress–strain measurements; the films were used for dynamic mechanical thermal analysis (DMTA).

Some of the polymers contained a small amount of talc. The talc content was determined with a Perkin–Elmer Model 7 TGA. The purge gas was oxygen. Specimens weighing between 10 and 15 mg were heated to 700°C at 10°C/min.

All DSC measurements were carried out in a Rheometrics DSC. Specimens weighing between 5 and 10 mg were treated as follows: heated from −80 to 180°C at a rate of 10°C/min (first heating), held at 190°C for 3 min, cooled to −80°C at 10°C/min, held at −80°C for 3 min, and reheated from −80 to 180°C at 10°C/min (second heating). The crystallinity (wt %) was calculated from the second heating using a heat of fusion of 290 J/g for the polyethylene crystal.

The density of small pieces cut from the plaques was measured according to ASTM D1505-85. For materials with density between 0.8 and 1.0 g/cm^3, an isopropanol–water density gradient column was used. For materials with density higher than 1.0 g/cm^3, an isopropanol–diethylene glycol column was used. Although the talc content was less than 2.5 wt %, the small amount significantly affected the density. The talc contribution was subtracted using the talc content determined by TGA and a talc density of 2.7 g/cm^3. The density corrected for talc is reported in Table II.

Dynamic mechanical measurements were made with a DMTA MkII unit from Polymer Laboratories operating in the tensile mode. The specimen dimensions were 0.5 × 7.0 × 13 mm. The tensile strain was less than 0.2%. The relaxation spectrum was scanned from −150°C through the glass transition with a frequency of 1 Hz and heating rate of 3°C/min. Subsequently, beginning 20°C below the glass transition temperature, the glass transition region was scanned with 5 frequencies (0.3, 1, 3, 10, and 30 Hz) with a heating rate of 0.2°C/min to determine the activation energy for the glass transition process. The glass transition temperature was taken as the maximum in the tan δ curve.

The stress–strain behavior in uniaxial tension was measured with ASTM 1708 microtensile

specimens cut from the plaques. A pattern was coated on the specimens by depositing 200 Å of gold over a square grid. Specimens were stretched in an Instron at 3 strain rates (10, 100, and 1000%/min). The grip separation was 22.25 mm, which included the fillet section. Engineering strain was calculated from the crosshead displacement. Engineering stress was defined conventionally as the force per initial unit cross-sectional area. During deformation, the pattern in the middle of the specimen was recorded with a video camera equipped with a telescopic lens. The draw ratio was defined as the deformed length of the square grid divided by the initial length.

RESULTS AND DISCUSSION

Crystallinity

The thermal behavior of 6 ESIs is illustrated with first and second heating thermograms in Figure 1. The 3 polymers with lowest styrene content showed a very broad melting endotherm beginning at about 0°C. With increasing styrene content, the peak melting temperature decreased, and the melting enthalpy decreased. These trends reflected the progressive decrease in length and number of crystallizable ethylene sequences. The first heating thermograms always contained an additional peak at about 35°C that was absent from the second heating thermograms. EO copolymers also exhibit this phenomenon.[11] Because the melting range extends below ambient temperature, the copolymers slowly recrystallize upon standing. This feature of ambient temperature annealing did not affect the measured melting enthalpy.

Figure 2 shows the decrease in DSC crystallinity with increasing styrene content. The dependence on comonomer content coincided with that of EO copolymers prepared with the INSITE™ technology. The maximum comonomer content for crystallization of about 20% is similar in other ethylene copolymers, such as ethylene–hexene and ethylene–vinyl acetate.[12,13] If the comonomer can enter the crystal lattice, such as in ethylene–propylene and ethylene–vinyl chloride copolymers, compositions in excess of 20 mol % comonomer can exhibit crystallinity.[13]

It has been suggested that the heat of melting is related to the mole percent ethylene (X_e) by the equation

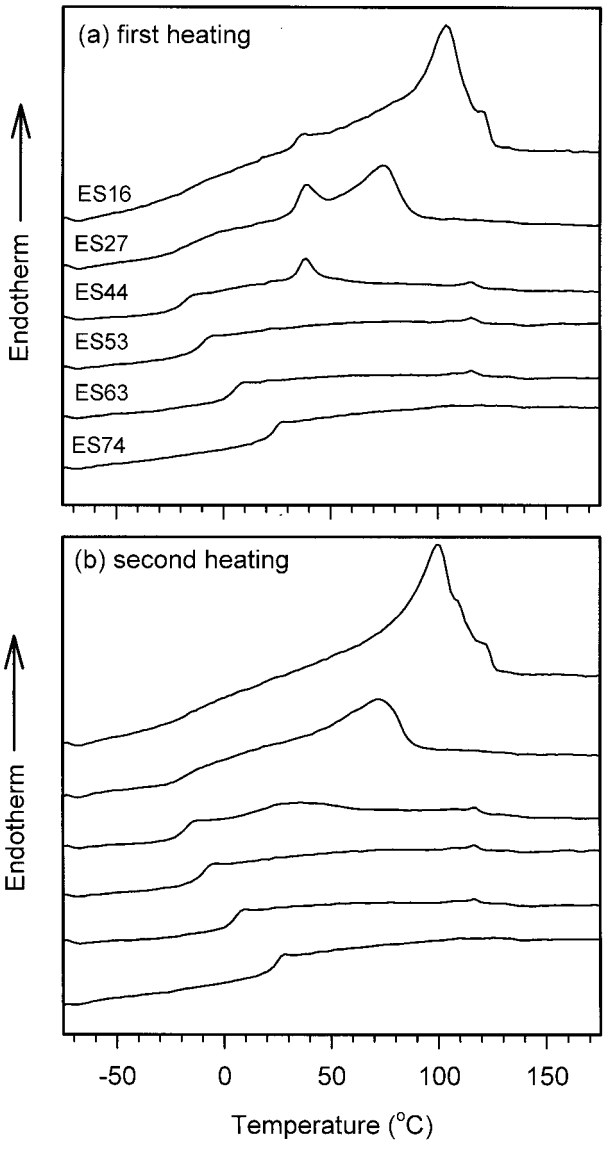

Figure 1 Melting thermograms of ESIs: (a) first heating and (b) second heating. The polymers are described in Table I.

$$\Delta H_m = \mathrm{k}(X_e)^n \quad (1)$$

where the constant k is related to the crystallinity of the homopolymer, and the exponent n is the minimum ethylene sequence length that can crystallize.[14] A linear relationship between log ΔH_m and log X_e is observed for many ethylene copolymers although the value of n depends on thermal history and chain characteristics. Because eq. (1) is derived from probability arguments, n is expected to depend on the ethylene sequence distribution, which, in turn, is determined by the

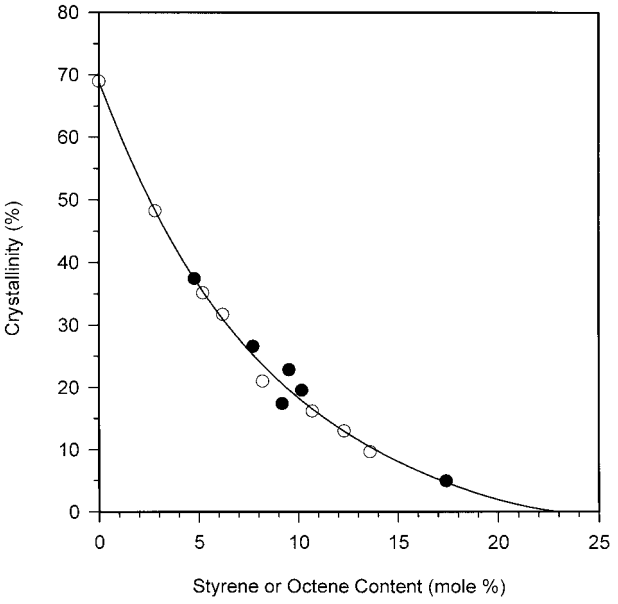

Figure 2 Crystallinity from DSC as a function of comonomer content. Data for ESIs (filled circles) are corrected for aPS and talc. Data for EO copolymers (open circles) are from Bensason et al.[10]

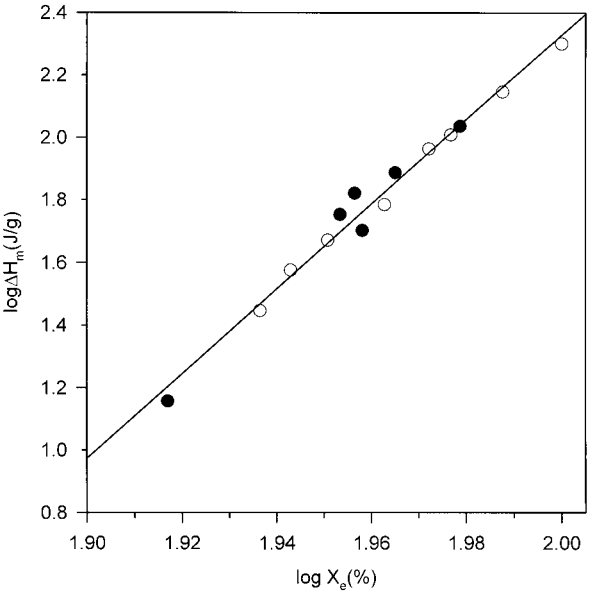

Figure 3 Logarithmic plot of the DSC heat of melting versus mole percent ethylene for ESIs (filled circles) and EO copolymers (open circles). The solid line has a slope of 13. Data for EO copolymers are from Bensason et al.[10]

comonomer, the catalyst system, and the polymerization conditions. Nevertheless, within a series of copolymers prepared by similar means with the same comonomer, the applicability of eq. (1) is usually confirmed. The data for ESIs corrected for aPS and talc are plotted in Figure 3. Data for EO copolymers are included for comparison; the solid line with $n = 13$ represents the best fit of the EO data.[10] Correspondence in the relationship between ΔH_m and X_e for the 2 series of polymers suggests that, at low comonomer contents, any differences in the distribution of comonomer units are not sufficient to affect the total ethylene in crystallizable sequences.

The relationship between density, after the talc contribution was removed, and total styrene content is shown in Figure 4. The solid line represents the linear relationship between density and composition based on a density of 1.065 g/cm^3 for atactic polystyrene and 0.855 g/cm^3 for amorphous polyethylene. The amorphous materials conformed well with the additivity rule. The density of the semicrystalline polymers lay above the linear relationship and was essentially independent of composition with a value of about 0.94 g/cm^3. Apparently, as the styrene content decreased, the increasing crystallinity compensated for the decreasing density of the amorphous phase.

To calculate the crystallinity from the measured density, the following two-phase model is assumed: a crystalline polyethylene phase, and an amorphous phase that consists of noncrystalline polymer and any atactic polystyrene. The

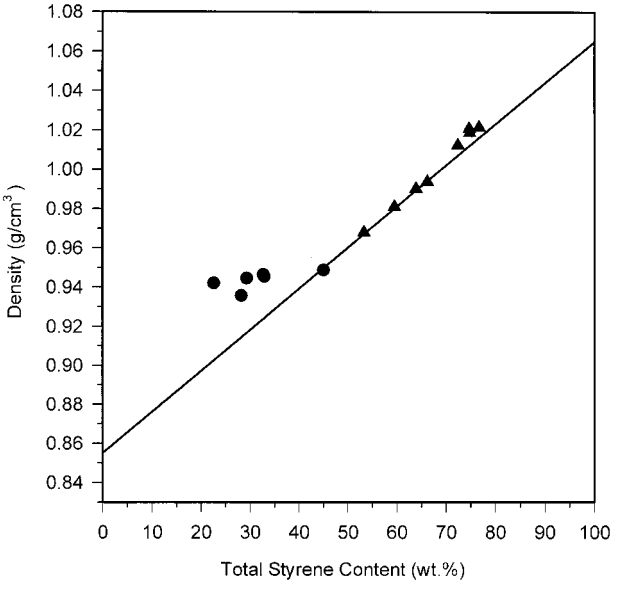

Figure 4 Measured density as a function of styrene content for semicrystalline (filled circles) and amorphous (filled triangles) ESIs.

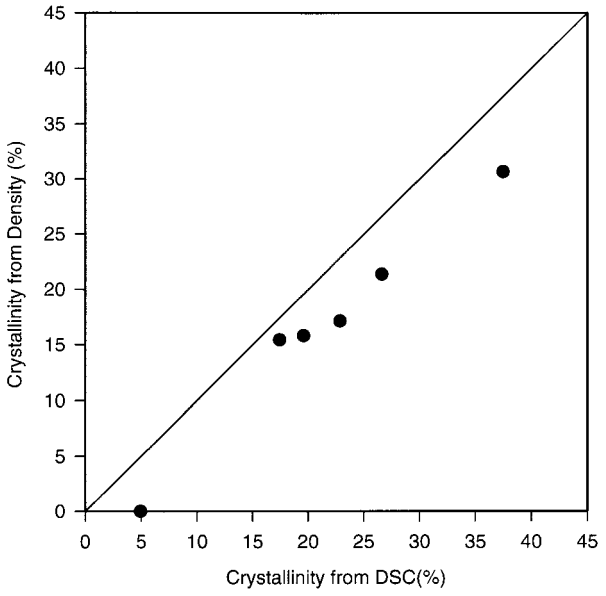

Figure 5 Percent crystallinity from density versus percent crystallinity from DSC melting enthalpy.

weight percent crystallinity W_x can then be expressed as

$$W_X = \frac{\rho_c(\rho - \rho_1)}{\rho(\rho_c - \rho_1)} \tag{2}$$

where ρ is the measured density of the polymer, ρ_c is the density of crystalline polyethylene (1.000 g/cm^3) and ρ_1 is the density of the amorphous phase. The density of the amorphous phase is assumed to be linear with styrene content and is given by

$$\rho_1 = \frac{W_e - W_X}{100 - W_X}\rho_a + \frac{100 - W_e}{100 - W_X}\rho_s \tag{3}$$

where ρ_a is the density of amorphous polyethylene, ρ_s is the density of polystyrene, and W_e is the weight percent ethylene.

The crystallinity calculated from eqs. (2) and (3) is compared in Figure 5 with the crystallinity obtained from the enthalpy of melting. The density calculation yields a very similar dependency on styrene content as the enthalpy calculation. For a wide variety of polyethylenes and ethylene copolymers, it has been found that density consistently gives a crystallinity about 10% higher than enthalpy. The difference is usually accounted for by considering a transition layer between the crystalline core and the amorphous regions.[15,16] An exception is the homogeneous EO copolymers prepared by the INSITE™ technology, where the equivalence of the 2 crystallinity determinations is observed.[10] In contrast, the density of ESIs gives a crystallinity about 5% lower than enthalpy. The unusual relationship between the 2 methods is probably due to shortcomings of the density model rather than to some unusual characteristic of the crystalline morphology.

Glass Transition

The DSC thermograms of noncrystalline ESIs exhibited a glass transition that decreased in temperature from about 25 to −20°C as the styrene content decreased. When the styrene content was low enough for the polymer to crystallize, the DSC glass transition broadened to the extent that it was difficult to resolve in the thermogram of the most crystalline polymers. The glass transition was more readily observed in the DMTA. The dynamic mechanical relaxation spectra of 6 representative ESIs are shown in the form of the storage modulus and loss tangent in Figure 6. The plots show the glass transition of the noncrystalline polymers as a sharp drop in modulus of about 3 orders of magnitude and a sharp peak in the loss tangent curve. The temperature of the loss tangent peak at 1 Hz was about 8°C higher than the DSC glass transition temperature. The glass transition temperature gradually shifted from slightly above ambient temperature to below ambient temperature as the styrene content decreased. When the styrene content was low enough for the polymer to crystallize, the loss tangent peak broadened, and the peak shifted to a slightly higher temperature. The smaller drop in modulus at the glass transition temperature and the higher modulus above the glass transition temperature in the semicrystalline polymers compared to the amorphous ones reflected the reinforcing effect of the crystalline phase.

The dependence of glass transition temperature on composition of random copolymers is usually described by the Fox equation or the Gordon–Taylor equation,

$$T_g = \frac{w_1 T_{g,1} + k w_2 T_{g,2}}{w_1 + k w_2} \tag{4}$$

where T_g is the measured glass transition temperature and w_i and $T_{g,i}$ refer to the weight fraction and glass transition temperature of component i. The natural approach in analyzing the

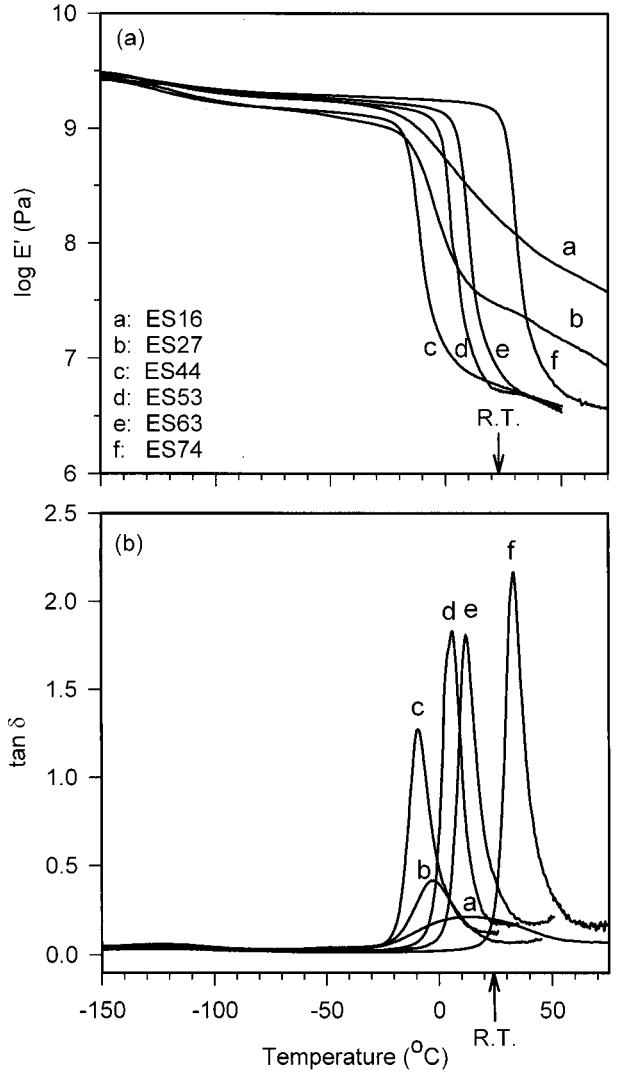

Figure 6 Dynamic mechanical relaxation behavior: (a) log E'; (b) tan δ.

ESIs is to take polystyrene and polyethylene as the homopolymers. However, attempts to fit the data resulted in an unrealistic value of 0.14 for the constant k in eq. (4), rather than a value close to unity.[9,17] The ESIs do not meet the assumption of randomness because styrene–styrene dyads are not allowed. Therefore, it is more appropriate to consider them as random copolymers of ethylene and ethylene–styrene dyads. The data in Figure 7 satisfactorily fit the Fox equation in the following form:

$$\frac{1}{T_g} = \frac{(1 - 1.27w_s)}{T_{g,e}} + \frac{1.27w_s}{T_{g,es}} \qquad (5)$$

where $T_{g,e}$ is the glass transition of polyethylene, $T_{g,es}$ is the glass transition of the alternating ethylene–styrene copolymer, and w_s is the weight fraction of styrene incorporated into the copolymer. Extrapolation gave a glass transition temperature of −66°C for amorphous polyethylene and 44°C for the alternating copolymer, which would have a composition of 79 wt % styrene. Equation (5) is a special case of the more general relationship between glass transition temperature and comonomer sequence distribution.[18–20] The data also fit a linear regression well, and extrapolation gave a glass transition temperature of −91°C for amorphous polyethylene and 40°C for the alternating copolymer of ethylene and styrene.

Crystallinity caused the tan δ peak to decrease in intensity and to broaden as the peak shifted to a higher temperature. The magnitude of the accompanying modulus drop correspondingly decreased. Contributing effects of the crystallinity included decreased volume fraction of the amorphous phase, restricted mobility of the amorphous chain segments by the crystalline domains, and higher styrene content of the amorphous phase due to segregation of styrene into the amorphous phase.

The frequency dependence of the tan δ peak temperature is shown in Figure 8 for the amor-

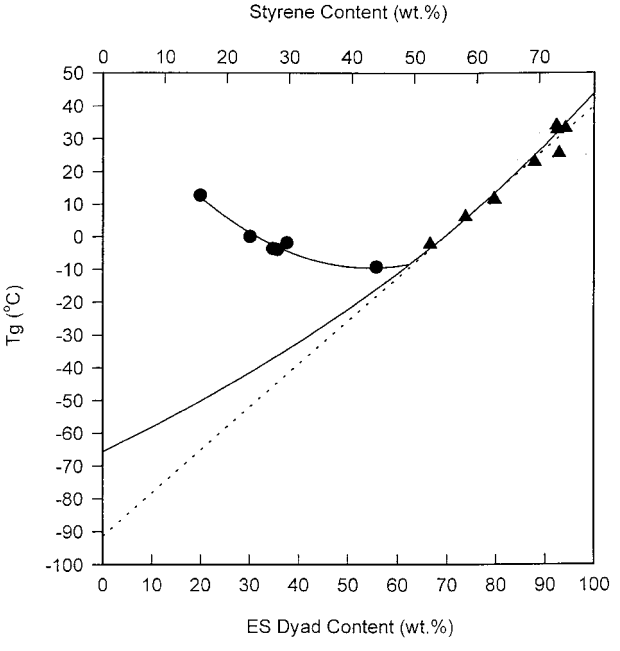

Figure 7 Glass transition temperature (tan δ, 1 Hz) as a function of weight percent ethylene–styrene dyads for semicrystalline (filled circles) and amorphous (filled triangles) ESIs. A solid line describes the fit with the Fox equation [eq. (5)]; the dotted line defines the linear relationship.

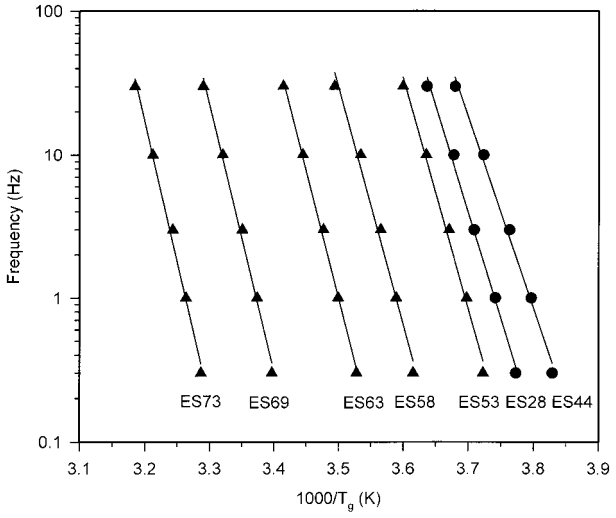

Figure 8 Arrhenius plots of the loss tangent peak temperature for representative semicrystalline (filled circles) and amorphous (filled triangles) ESIs.

phous and semicrystalline ESIs. The Arrhenius plots were linear for all compositions, and the corresponding activation energies are included in Table II. The activation energy for the glass transition of the amorphous polymers decreased linearly with wt % ethylene–styrene dyads. The linear relationship extrapolated to 393 kJ/mol for the alternating copolymer and to 126 kJ/mol for amorphous polyethylene, a value that compares to 180 kJ/mol for the activation energy of the polyethylene β relaxation.[21]

Stress–Strain Behavior

The correspondence in Figure 9 between the engineering strain and the local draw ratio taken from a grid marked on the specimen indicated that all the polymers deformed uniformly without localized necking at ambient temperature. The slight deviation above the dotted line at intermediate strains was due to the slight constraint at the ends of the dogbone-shaped specimen; deviation below the line at high strains indicated that material was pulling out from the grips.

The stress–strain curves of a semicrystalline ESI at 3 strain rates are shown in Figure 10(a). The deformation has elastomeric characteristics with a low initial modulus, a plateau region followed by strain hardening, and large instantaneous strain recovery following fracture. This is very similar to the behavior of low-crystallinity (type I) EO copolymers.[10] The concept of a network of flexible chains with fringed micellar crystals serving as multifunctional junctions provides the structural basis for the elastic behavior of EO copolymers.[22] The model may also be appropriate for ESIs with crystallinities of approximately 20% or less. Insensitivity of the stress–strain curve to strain rate reinforces the analogy with type I EO copolymers. However an important difference concerns the lower glass transition temperature of EO copolymers compared to ESIs, approximately −40°C compared to −4°C. It can be anticipated that EO copolymers retain elastomeric characteristics to lower temperatures than ESIs.

The amorphous ESIs did not possess a reinforcing crystalline phase, and, consequently, the glass transition temperature primarily determined the stress–strain behavior. The glass transition of the amorphous polymers increased with styrene content over a temperature range that spanned ambient temperature. As a result, the stress–strain behavior strongly depended on composition and also exhibited strong rate effects. The stress–strain curves in Figure 10(b) are for an ESI with 63 wt % styrene that was slightly above the glass transition temperature (T_g = 11°C). Without the reinforcing effect of crystals, the initial modulus and the total stress response were much lower than those of the semicrystalline polymer [Fig. 10(a)]. Furthermore, the glass transition was close enough to ambient temperature for strain rate to significantly affect the stress–strain behavior. At the highest strain rate,

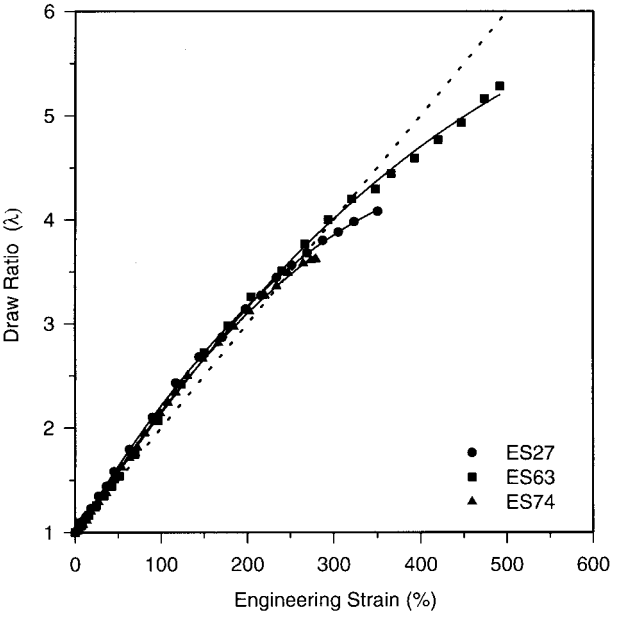

Figure 9 Draw ratio versus engineering strain.

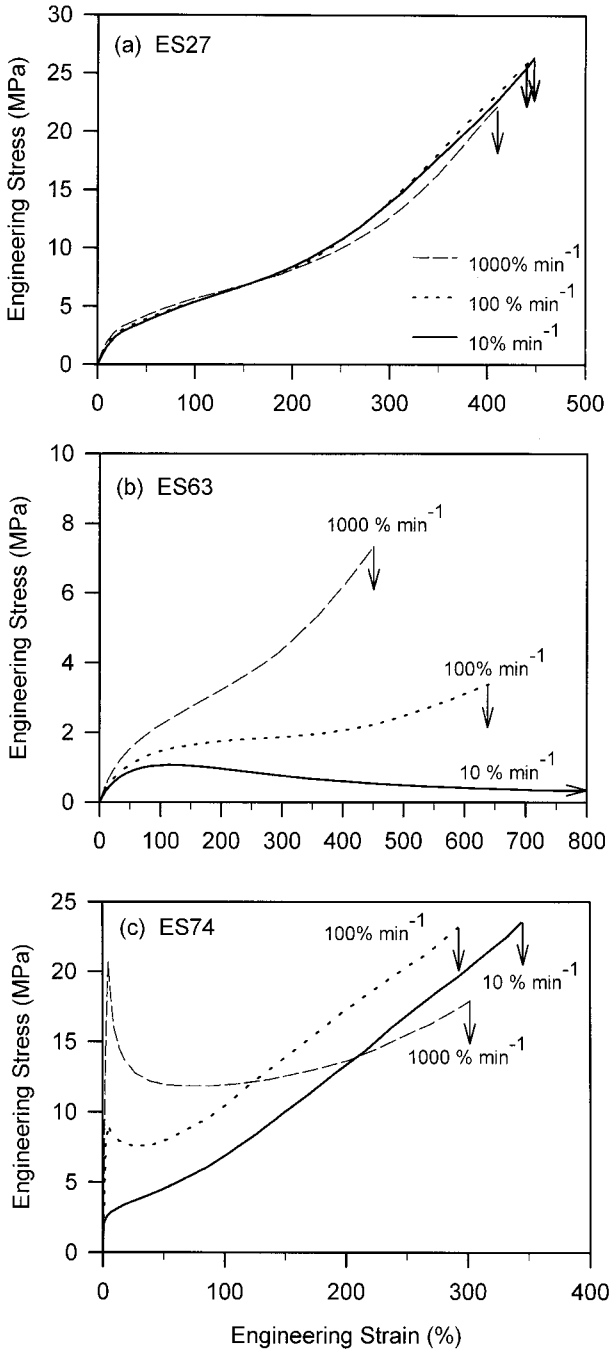

Figure 10 Engineering stress–strain curves at 3 strain rates: (a) ES27; (b) ES63; (c) ES74.

1000%/min, the polymer exhibited rubbery behavior with strain hardening. Because the polymer did not possess permanent crosslinks, the elasticity was attributed to the entanglement network.[23] When stretched at the lowest rate, 10%/min, the polymer exhibited strain softening. This type of material is sometimes described as a rubber-like liquid.[24,25]

The stress–strain behavior of an amorphous ESI that was below the glass transition temperature (T_g = 33°C) is shown in Figure 10(c). The sharp stress maximum at low strains increased in prominence as the strain rate increased. This maximum was not associated with localized thinning or necking of the specimen; on the contrary, the polymer deformed uniformly at all strain rates. The maximum was a manifestation of the large strain rate dependence of the modulus at temperatures close to the glass transition temperature.[26,27] Because this polymer was just below the glass transition temperature, it initially exhibited glassy behavior at high strain rates, as indicated by the high initial modulus. However, the stress dropped as the polymer rapidly relaxed, thus producing the maximum. The stress maximum was less prominent at a strain rate of 100%/min than at 1000%/min, and, at a rate of 10%/min, it was not detectable.

The ambient temperature stress–strain behavior of 6 ESIs is compared in Figure 11 with a strain rate of 100%/min. These 6 polymers span the range in styrene content used in this study. The modulus, fracture stress, and fracture strain of all the polymers are included in Table II. Three types of behavior are easily distinguished. The semicrystalline polymers showed typical elastomeric behavior (ES28 and ES44): The initial modulus was intermediate among the polymers and was followed by a plateau region and a long strain

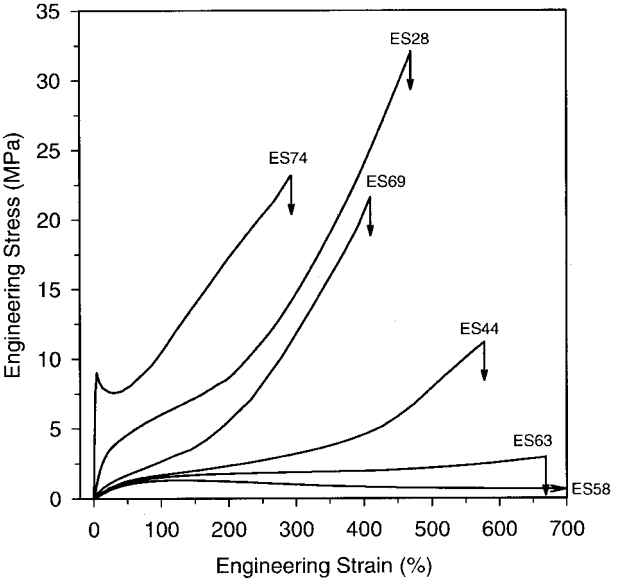

Figure 11 Engineering stress–strain curves of representative ESIs at a strain rate of 100%/min.

hardening region of gradually increasing stress response. Polymers with styrene content greater than 50 wt % did not crystallize. Between 50 and 70 wt % styrene, the glass transition was below ambient temperature. Polymers in this category exhibited the lowest initial modulus (ES58, ES63, and ES69). If the glass transition temperature was well below ambient temperature, they flowed to virtually infinite strains. As the glass transition approached ambient temperature, the behavior became more thermoplastic-like with increasing strain hardening and gradually decreasing fracture strain. Polymers with more than 70 wt % styrene had a glass transition temperature above ambient temperature. They typically exhibited a high glass-like initial modulus and a characteristic stress maximum due to relaxation (ES74). The fracture strain of these polymers, in the range of 300%, was the lowest of the ESIs but was higher than that of many glassy polymers.

Classification of Ethylene–Styrene Interpolymers

The combined observations from melting behavior, dynamic mechanical response, and stress–strain behavior suggest a classification scheme with 3 categories (Fig. 12). A composition of approximately 50 wt % styrene separates the semicrystalline polymers from the amorphous ones. The crystalline polymers are identified as type E. They melt over a broad temperature range, which begins at about 0°C and can extend as high as 100°C for polymers with lower styrene content. The stress–strain curve at ambient temperature is not sensitive to strain rate and exhibits other elastomeric characteristics, including a low initial modulus, a gradual increase in the slope of the stress–strain curve at higher strains, and large instantaneous recovery. The elastomeric stress–strain behavior of type E ESIs with 20–50 wt % styrene compares with that of type I EO copolymers.[10] The structural origins of the elastomeric behavior may be similar. The concept of a network of flexible chains with fringed micellar crystals serving as the multifunctional junctions provides the structural basis for analyzing the elastomeric characteristics of EO copolymers.[22] A primary difference between elastomeric EO copolymers and ESIs is the glass transition temperature of the network chain segments. This depends on the chemical structure of the comonomer. The glass transition of the ESIs with the bulky styrene group is about 40°C higher than that of the EO copolymers.

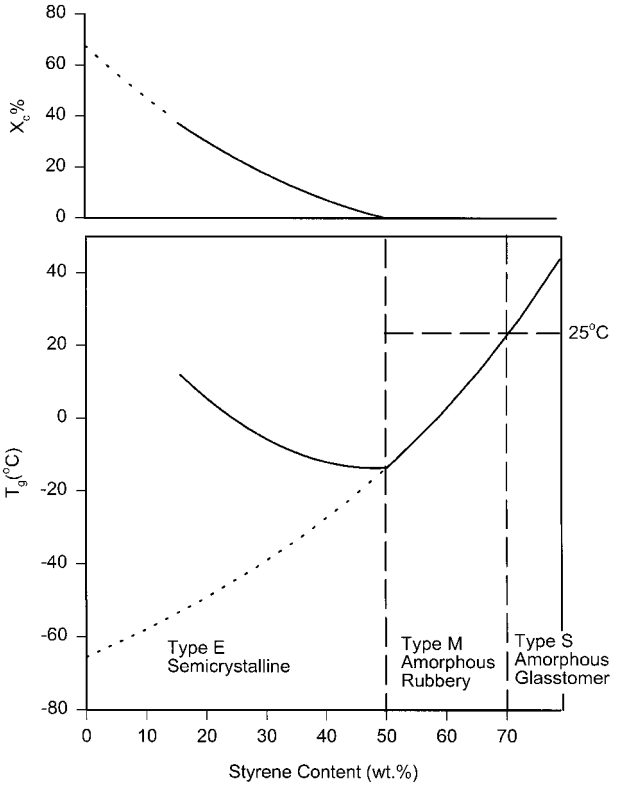

Figure 12 Classification scheme of ESIs based on composition.

Polymers with more than 50 wt % styrene are amorphous. The composition dependence of physical properties, such as density and glass transition temperature, conforms with well-established relationships. However, because the span in glass transition temperature encompasses ambient temperature, it is useful to differentiate between polymers that are above the glass transition temperature and those that are below as type M and type S, respectively. At ambient temperature, type M polymers are those with 50 to 70 wt % styrene. They have the lowest modulus and lowest stress levels of the ESIs. Because the polymer does not possess permanent crosslinks, elastic characteristics are attributed to the entanglement network. Type S polymers are below their glass transition temperature at ambient temperature. However, they are only slightly below the T_g, and, therefore, their mechanical response is very rate-dependent. They exhibit glassy behavior at short times and rubbery behavior at longer times. The term "glasstomer" is coined to describe this particular class of polymers. The division between type M and type S is based on chain dynamics, rather than solid state structure, and,

thus, will shift to a higher or lower styrene content, depending on the temperature of interest.

The authors thank the Dow Chemical Company for financial support.

REFERENCES

1. K. Soga, D. Lee, and H. Yanagihara, *Polym. Bull.,* **20,** 237 (1988).
2. P. Aaltonen and J. Seppälä, *Eur. Polym. J.,* **30,** 683 (1994).
3. P. Aaltonen, J. Seppälä, L. Matilainen, and M. Leskelä, *Macromolecules,* **27,** 3136 (1994).
4. T. Miyatake, K. Mizunuma, and M. Kakugo, *Makromol. Chem., Macromol. Symp.,* **66,** 203 (1993).
5. J. Ren and F. R. Hatfield, *Macromolecules,* **28,** 2588 (1995).
6. G. Xu and S. Lin, *Macromolecules,* **30,** 685 (1997).
7. Y. W. Cheung and M. J. Guest, in *ANTEC '96 SPE Conference Proceedings,* 1996, pp. 1634–1637.
8. K. W. Swogger and S. P. Chum, in *MetCon '97 "Polymers in Transition" Conference Proceedings,* 1997.
9. S. F. Mudrich, Y. W. Cheung, and M. J. Guest, in *ANTEC '97 SPE Conference Proceedings,* 1997, pp. 1783–1787.
10. S. Bensason, J. Minick, A. Moet, S. Chum, A. Hiltner, and E. Baer, *J. Polym. Sci., Part B: Polym. Phys.,* **34,** 1301 (1996).
11. J. Minick, A. Moet, A. Hiltner, E. Baer, and S. P. Chum, *J. Appl. Polym. Sci.,* **58,** 1371 (1995).
12. I. O. Salyer and A. S. Kenyon, *J. Polym. Sci., Part A-1,* **9,** 3083 (1971).
13. S. Hosoda, *Polym. J.,* **20,** 383 (1988).
14. D. R. Burfield, *Macromolecules,* **20,** 3020 (1987).
15. R. Alamo, R. Domszy, and L. Mandelkern, *J. Phys. Chem.,* **88,** 6587 (1984).
16. F. Defoor, G. Groeninckx, P. Schouterden, and B. Van der Heijden, *Polymer,* **33,** 5186 (1992).
17. A. Lobbrecht, Chr. Friedrich, F. G. Sernetz, and R. Mülhaupt, *J. Appl. Polym. Sci.,* **65,** 209 (1997).
18. M. Hirooka and T. Kato, *Polym. Lett.,* **12,** 31 (1974).
19. N. W. Johnston, *J. Macromol. Sci., Rev. Macromol. Chem.,* **C14,** 215 (1976).
20. H. Suzuki, N. Kimura, and Y. Nishio, *J. Therm. Anal.,* **46,** 1011 (1996).
21. J. Brandrup and E. H. Immergut, Eds., *Polymer Handbook,* Wiley, New York, 1989, V-22.
22. S. Bensason, E. V. Stepanov, S. Chum, A. Hiltner, and E. Baer, *Macromolecules,* **30,** 2436 (1997).
23. R. Muller, D. Froelich, and Y. H. Zang, *J. Polym. Sci., Part B: Polym. Phys.,* **25,** 295 (1987).
24. M. H. Wagner and J. Meissner, *Makromol. Chem.,* **181,** 1533 (1980).
25. C. W. Macosko, in *Rheology: Principles, Measurements, and Applications,* C. W. Mocosko, Ed., VCH Publishers, New York, 1994, p. 45.
26. C. Bauwens-Crowet, J. C. Bauwens, and G. Homès, *J. Polym. Sci., Part A-2,* **7,** 735 (1969).
27. J. C. Bauwens, C. Bauwens-Crowet, and G. Homès, *J. Polym. Sci., Part A-2,* **7,** 1745 (1969).